COMMENTS AND FURTHER ANALYSIS ON EFFECTIVE ROUGHNESS LENGTHS FOR USE IN NUMERICAL THREE-DIMENSIONAL MODELS

(Research Note)

PETER A. TAYLOR

Boundary-Layer Research Division, Atmospheric Environment Service, Downsview, Ontario, Canada M3H 5T4

(Received in final form 9 February, 1987)

Abstract. Simple calculations of the apparent roughness length for the areally averaged flow over flat but heterogeneous terrain are presented. These results could be used to specify effective roughness lengths for use in large-scale models. Some of our conclusions differ significantly from those reached recently by André and Blondin (1986).

1. Introduction

In their recent paper, André and Blondin (1986) consider the parameterization of heterogeneous terrain in large-scale models using the concept of an effective roughness length, z_0^{eff}. Their results suggest that z_0^{eff} is significantly different from the value one would obtain from a spatial average of the logarithm of the local micrometeorological roughness lengths over a model grid square and that it is strongly dependent upon the height of the first level, z_1, of the model being used. We shall argue against any dependence on z_1 and suggest that,

$$z_0^{\text{eff}} \simeq z_{0m} \tag{2}$$

where

$$\ln z_{0m} = \langle \ln z_0 \rangle ,$$

and $\langle\ \rangle$ implies a grid-square average, is usually a reasonable approximation. We also propose a first-order correction based on PBL similarity theory and discuss various alternative approaches to the definition of z_0^{eff}. As large- and meso-scale numerical models develop, it may be found necessary to improve on this and we can perhaps use high-resolution models to guide in the representation of sub-grid scale effects or even to produce 'grid-square specific' parameterizations. At the present time, however, estimates of z_0^{eff} within a factor 2 are probably adequate and such considerations may be premature.

2. The Problem

André and Blondin simplify their analysis by considering only neutral stratification and assuming that z_1 is sufficiently close to the ground for the local velocity profiles to be

Boundary-Layer Meteorology **39** (1987) 403–418.

logarithmic of the form

$$u = \frac{u_*}{k}(\ln z - \ln z_0)\,. \tag{2}$$

We shall do the same and also assume, as they do, that the heterogeneous grid square is flat and consists of a patchwork of areas (or 'patchwork quilt') of different roughness. Then, although $z_0 = z_0(x, y)$, the local profiles will be of the form (2) except in narrow transition areas between different regions. These areas should only have a small contribution to the average. An alternative might be to assume slow spatial variations in z_0 so that profiles are always in approximate local equilibrium. Averaging Equation (2) over the grid square gives

$$\langle u(z) \rangle = \frac{1}{k}[\langle u_* \rangle \ln z - \langle u_* \ln z_0 \rangle]\,. \tag{3a}$$

This average profile is logarithmic in z but:

(a) the apparent friction velocity $\langle u_* \rangle$ is not necessarily equal to the square root of the average stress $\langle u_*^2 \rangle$ and

(b) the apparent roughness length is not simply related to the local roughness length distribution but also depends to some extent on the u_* distribution. Denoting the 'apparent roughness length' by z_{0a}, we would have

$$\ln z_{0a} = \langle u_* \ln z_0 \rangle / \langle u_* \rangle \tag{3b}$$

in order that

$$\langle u(z) \rangle = \frac{\langle u_* \rangle}{k}(\ln z/z_{0a})\,. \tag{4}$$

In general we suggest setting $z_0^{\text{eff}} = z_{0a}$ but wish to distinguish between the two on a conceptual basis at this time.

A very simple case is that of a 'half and half' grid square with $z_0 = z_{0s}$ in the smooth half and z_{0r} in the rough. Figure 1 shows schematic profiles of u vs $\ln z$ for this situation. In drawing this graph, we do not know the relationship between the u_r and u_s profiles but have sketched them on the basis that, given the same driving force generating the profiles over the rough and smooth surfaces, we would expect $u_s(z) > u_r(z)$. Key questions are:

What should be considered as the driving force? and

Is it uniform over the grid square?

André and Blondin, in Section 2 of their paper, assume that u is fixed, and equal to u_1 at $z = z_1$. In our example, this would imply $u_{1r} = u_{1s}$. If z_1 is large, say $O(200\text{ m} +)$, this may be an acceptable assumption but it is not appropriate for $z_1 \sim 10$ m. For heights in this range, we know from everyday experience that winds are reduced over rougher surfaces. In our view then, it is inappropriate to regard the wind speed at some height

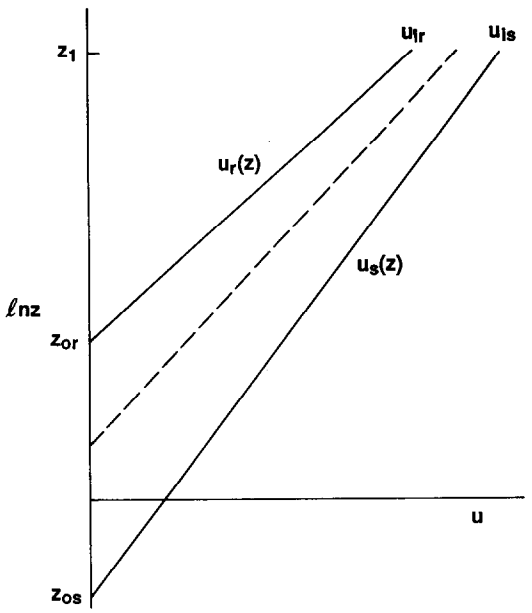

Fig. 1. Schematic diagram of velocity profiles above a 'half-and-half' grid square: ——— 'rough' and 'smooth' profiles, u_r, u_s; – – – – – grid-square average profile $\langle u(z) \rangle$.

within the surface layer as providing the driving mechanism for the near surface boundary-layer flow since it will not be uniform over the grid square.

3. A Better Way?

For studies of surface boundary-layer flow above variations in roughness where the upstream or unperturbed flow is a constant stress layer, the appropriate upper boundary condition and driving force is one of a constant applied shear stress (see, for example, Taylor, 1969a). This is not strictly appropriate here but note that it would lead to equilibrium profiles above different roughnesses all having the same value of u_* and, hence, $\ln z_{0a} = \ln z_{0m}$.

For situations considered by GCMs and synoptic and regional scale NWP models, we can reasonably expect that horizontal pressure gradients, on the synoptic- or meso-scale, will vary only slowly across a grid square and will be relatively unaffected by sub-grid scale variations in surface properties. If this is the case, our sub-grid scale problem becomes one of representing the average planetary boundary layer (PBL) over heterogeneous terrain. In this case, the driving force is the externally imposed pressure gradient and the upper boundary condition, as $z \to \infty$, could either be one of zero stress or, equivalently, requiring that $\mathbf{u} \to \mathbf{u}_g$, the gradient or geostrophic wind in balance with the pressure gradient. Taylor (1969b) and Jensen (1978) have considered this situation for a simple step change in roughness and neutral conditions. Both analyses give similar

results and show that, following a step change in roughness, the surface friction velocity at first overshoots the new equilibrium value for the downstream surface and then slowly adjusts back towards it. Complete adjustment of the flow to the new surface conditions appears to take a distance of $O(V_g/f)$, where f is the Coriolis parameter and $V_g = |\mathbf{u}_g|$. This is typically ~ 100 km and Jensen (1978) uses this to argue that the PBL is rarely in equilibrium with the surface boundary. We accept this but note that u_* and the near surface wind speeds adjust rather faster than wind directions and speeds higher up in the boundary layer; we also note that the results indicate that surface friction velocities should almost always be within 5% of their equilibrium downstream values within a fetch of 10 km. On this basis and in the present context, we shall assume that the PBL transition zones are small relative to the sizes of individual areas in our patchwork quilt.

4. A Relationship for z_{0a}

If then, the surface stress is assumed to adjust fairly rapidly to changes in z_0, the implication is that we can estimate the relationship between u_* and $\ln z_0$ (needed for Equation (3b)) from models or theories of the PBL over homogeneous terrain. This has been investigated fairly extensively, especially on the basis of Ekman layer similarity theory and 'resistance laws' (see, for example, McBean, 1979). A graph of u_*/V_g as a function of $\ln \mathrm{Ro}$ (where Ro is the roughness Rossby number V_g/fz_0) based on this theory is given in Figure 2. Additional details are in Appendix 1. Note first that u_* varies relatively slowly with z_0 and, to a reasonable degree over limited ranges, can be approximated as varying linearly with $\ln z_0$. For fixed V_g and f, a suitable approximation would be

$$u_* = u_{*m}(1 + a_1(\ln z_0 - \ln z_{0m})), \tag{5}$$

where

$$a_1 = \left(\frac{1}{u_*}\frac{\mathrm{d}u_*}{\mathrm{d}(\ln z_0)}\right) \quad \text{at} \quad \ln z_0 = \ln z_{0m} \tag{6}$$

and u_{*m} is the value of u_* corresponding to $\ln z_0 = \ln z_{0m}$. With the assumed linear relationship, Equation (5), this will be equal to $\langle u_* \rangle$.

Substituting (5) into (3b) and assuming $u_{*m} = \langle u_* \rangle$ gives

$$\ln z_{0a} = \langle \ln z_0 \rangle + a_1(\langle (\ln z_0)^2 \rangle - (\langle \ln z_0 \rangle)^2) \tag{7a}$$

or

$$\ln z_{0a} = \langle \ln z_0 \rangle + a_1 \sigma^2_{\ln z_0}. \tag{7b}$$

The same result can be obtained, correct to $O(\Delta^3)$ where $\Delta = \ln z_0 - \ln z_{0m}$, by using a Taylor series expansion for u_* in place of Equation (5). Since $a_1 > 0$, the value of $\ln z_{0a}$ will always be $\geq \langle \ln z_0 \rangle$ but not by too much in many cases. Note that there is no dependence on z_1 in this analysis. As a simple illustration, consider a grid square with

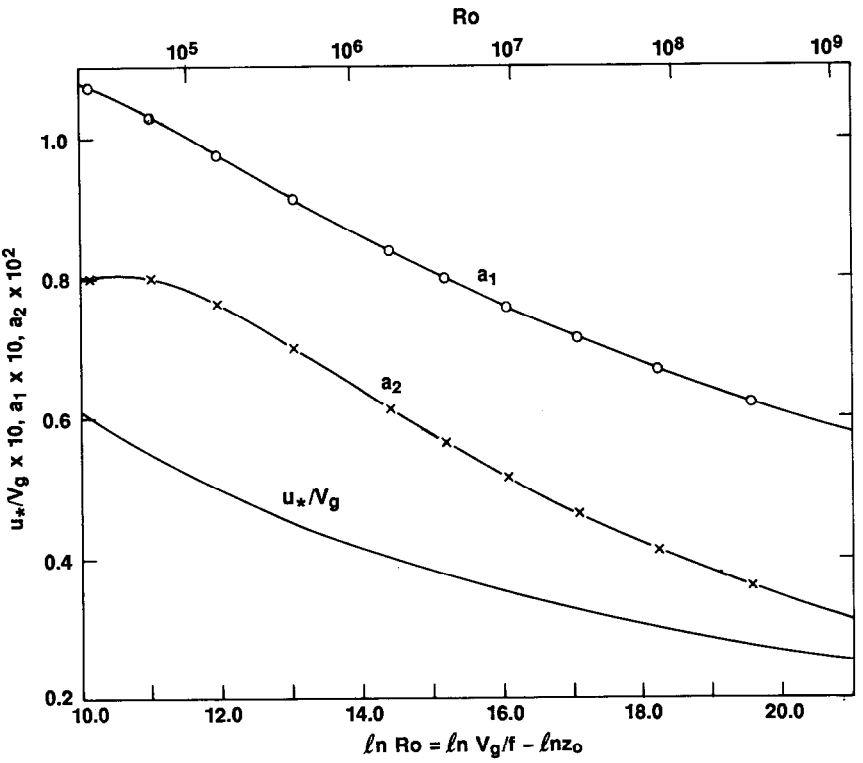

Fig. 2. The relationship between u_*/V_g and Ro for neutrally stratified PBL flow, based on similarity theory:

$$a_1 = \frac{1}{u_*}\frac{\mathrm{d}u_*}{\mathrm{d}(\ln z_0)}; \qquad a_2 = \frac{1}{2u_*}\frac{\mathrm{d}^2u_*}{\mathrm{d}(\ln z_0)^2}$$

See Appendix for additional details.

equal halves with $z_0 = 0.02$ and 0.5 m. Then, with $a_1 = 0.087$ (from the Appendix or Figure 2),

$$\ln z_{0a} = -2.303 + 0.087\,(7.89 - 5.30) = -2.078.$$

In this case, the value of z_{0m} corresponding to $\langle \ln z_0 \rangle$ is 0.1 m while $z_{0a} = 0.125$ m. Given all the other uncertainties and imperfections in the parameterization of the boundary layer within large-scale models, this seems a rather insignificant difference. However, it can be larger in cases with a wider range of surface roughness within a grid square. For the simple 'half and half' case, we have computed $\ln z_{0a}$ based both on Equation (7b) and from Equation (3b) using the full PBL similarly theory relationship (see Equation (A1)) between u_* and $\ln z_0$ for a number of cases. The results are given in Table 1 together with values of z_{0m}. It is clear in all cases that Equation (7b) provides an excellent approximation to the 'exact' solution based on Equations (3b) and (A1). The results also confirm our earlier assessment that z_{0m} should be adequate in most

cases. In the two extreme cases included where the ratio of rough-to-smooth roughness lengths, $z_{0r}/z_{0s} = 10^4$, the apparent z_0 is substantially increased ($\times 5$ and $\times 6$ in the two cases tabulated). This situation could arise in grid squares containing, for example, a mix of land and water surfaces or of forest and snow covered open ground. In these cases we suggest using Equation (7b) to determine z_{0a}. In other cases, the same equations could be used but the correction to the simpler Equation (1) is probably not significant for present large-scale models. Note also that although a_1 varies from 0.6 to 1.1 over the Ro range considered, we could get a reasonable estimate of z_{0a} by taking a constant value of 0.85 for a_1.

5. The Surface Stress

Returning to problem (a), we might ask whether our proposed approximation to $\ln z_{0a}$ can also provide an estimate of $\langle u_*^2 \rangle$. We know from the Schwartz inequality that $\langle u_*^2 \rangle \geq (\langle u_* \rangle)^2$; the question to be asked is whether or not the correction is significant in relation to other model errors.

We can see from averaging Equation (5) that differences between $\langle u_* \rangle$ and u_{*m} are second order in $(\ln z_0 - \ln z_{0m})$. The same will be true of differences between $\langle u_*^2 \rangle$ and $\langle u_* \rangle^2$ and in order to estimate these we must take an extra term in the expansion (5) to give

$$u_* = u_{*m}(1 + a_1(\ln z_0 - \langle \ln z_0 \rangle) + a_2(\ln z_0 - \langle \ln z_0 \rangle)^2) . \tag{8}$$

An equation for a_2 is given in the Appendix while values are shown in Figure 2. With this second-order term, we can also get an estimate for the error involved in assuming

TABLE I

Different estimates of z_0^{eff} and $\langle u_*^2 \rangle$ for 'half-and-half' grid squares

Ro[a]	z_{0r}/z_{0s}	Equation (1)		Equation (7)		Equation (3)	
		$\ln z_{0m}$	z_{0m} (m)	$\ln z_{0a}$	z_{0a} (m)	$\ln z_{0a}$	z_{0a} (m)
10^5	25	0	1.0	0.26	1.30	0.26	1.30
	10^2	0	1.0	0.53	1.70	0.52	1.68
10^6	25	−2.30	0.10	−2.08	0.12	−2.08	0.12
	10^2	−2.30	0.10	−1.84	0.16	−1.85	0.16
	10^4	−2.30	0.10	−0.46	0.63	−0.53	0.59
10^7	25	−4.60	0.01	−4.40	0.012	−4.41	0.012
	10^2	−4.60	0.01	−4.20	0.015	−4.21	0.015
	10^4	−4.60	0.01	−3.00	0.050	−3.04	0.048
10^8	25	−6.91	0.001	−6.74	0.0012	−6.73	0.0012
	10^2	−6.91	0.001	−6.56	0.0014	−6.55	0.0014

[a] Ro values based on $V_g = 10\ \text{m s}^{-1}$, $f = 10^{-4}\ \text{s}^{-1}$ and z_{0m}.

Table I (continued)

$\langle u_* \rangle / u_{*m}$		$\langle u_*^2 \rangle / \langle u_* \rangle^2$	
Equation (9)	Similarity theory	Equation (10)	Similarity theory
1.020	1.018	1.026	1.027
1.041	1.039	1.053	1.051
1.017	1.018	1.019	1.018
1.034	1.038	1.040	1.039
1.137	1.144	1.159	1.148
1.013	1.009	1.015	1.014
1.027	1.023	1.030	1.030
1.109	1.113	1.121	1.116
1.010	1.012	1.011	1.013
1.021	1.025	1.023	1.024

$\langle u_* \rangle = u_{*m}$. This is obtained by averaging Equation (8) over the grid square to give

$$\langle u_* \rangle = u_{*m}(1 + a_2 \sigma^2_{\ln z_0}) . \tag{9}$$

We can now square and average Equation (8), square Equation (9), divide and approximate to show that the ratio $\langle u_*^2 \rangle / (\langle u_* \rangle)^2$ is given, to second order, as

$$\langle u_*^2 \rangle = \langle u_* \rangle^2 (1 + a_1^2 \sigma^2_{\ln z_0}) . \tag{10}$$

Estimates of $\langle u_* \rangle / u_{*m}$ and $\langle u_* \rangle^2 / \langle u_*^2 \rangle$ based on these equations and the full similarity theory are given for 'half and half' grid squares in Table I. Differences between $\langle u_* \rangle$ and u_{*m} are small ($< 5\%$) except in the cases where $z_{0r}/z_{0s} = 10^4$, and even then they are $< 15\%$.

The ratio $\langle u_* \rangle^2 / \langle u_*^2 \rangle$ is always close to 1.0 for the cases considered and shows that possible errors in estimating surface stress as $\langle u_* \rangle^2$ could be expected to be negligible. If corrections are considered necessary, the estimate based on Equation (10) provides a good approximation to the full similarity theory calculation.

6. Alternative Approaches

We believe that (3b) is the most appropriate definition for z_0^{eff}. There are, however, other possibilities, based on the requirement that the assumed profiles will give the correct surface stress directly. This is indeed a useful feature and was incorporated in the original definition by Fiedler and Panofsky (1972). It does however have the disadvantages that the profile for $z < z_1$ is no longer equal to $\langle u(z) \rangle$ and the value of z_0^{eff} is dependent on the choice of z_1. Two alternative definitions, denoted here by z_{0b} and z_{0c} are based on the equations

$$\langle u_1 \rangle = \frac{\langle u_*^2 \rangle^{1/2}}{k} \left(\ln \frac{z_1}{z_{0b}} \right) \tag{11}$$

and

$$\langle u_1^2 \rangle^{1/2} = \frac{\langle u_*^2 \rangle^{1/2}}{k} \left(\ln \frac{z_1}{z_{0c}} \right). \tag{12}$$

With z_{0b} we could obtain the correct stress from a known $\langle u_1 \rangle$ while with z_{0c}, which is perhaps a little esoteric, we would need knowledge of $\langle u_1^2 \rangle$. If z_1 is sufficiently high that u_1 is uniform across the grid square, then z_{0b} and z_{0c} would be equivalent and would correspond to the value obtained by simply averaging the drag coefficients as suggested, for example, by Wieringa (1986, p. 874). This leads to yet another estimate of z_0^{eff}; the relationship can be written as

$$(\ln z_1/z_{0d})^{-2} = \langle (\ln z_1/z_0)^{-2} \rangle . \tag{13}$$

The analysis in Section 2 of André and Blondin's paper is based on a profile of the form (4) with $u_*^{\text{eff}} = \langle u_* \rangle$ (their Equation (6b)). Their z_0^{eff}, which we shall identify as z_{0e} satisfies

$$\left(\ln \frac{z_1}{z_{0e}} \right)^{-1} = \left\langle \left(\ln \frac{z_1}{z_0} \right)^{-1} \right\rangle ; \tag{14}$$

this is equivalent to their Equation (8).

We must stress that the formulations of both z_{0d} and z_{0e} assume a uniform u_1 and ignore variations of u_1 with z_0 within the grid square. In our view, this assumption may be defensible for $z_1 \sim 200$ m but will be less and less valid as z_1 decreases.

The wind speed at the lowest level in a large-scale model is presumably intended to represent the grid-square average value, $\langle u_1 \rangle$; the appropriate z_0^{eff} to give the correct surface stress directly would be z_{0b}. We can, after some algebra, relate this to z_{0a} through the relationship

$$\ln z_{0b} = \alpha \ln z_{0a} + (1 - \alpha) \ln z_1 \tag{15}$$

where

$$\alpha = \langle u_* \rangle / \langle u_*^2 \rangle^{1/2},$$

and will be ≤ 1 by the Schwartz inequality.

Equation (15) shows that z_{0b} will increase with increasing z_1 although in most cases the rate of increase will be slow since $\alpha \simeq 1$. By contrast, z_{0d} and z_{0e} both decrease as z_1 increases. Some comparisons between all of the different z_0^{eff} estimates discussed are given for half-and-half grid squares and $z_{0r}/z_{0s} = 10^2$ in Table II. In calculating z_{0a}, z_{0b}, and z_{0c}, we have assumed that the local u_* and z_0 values are related through similarity theory as illustrated in Figure 2 and discussed in the Appendix. We can see that the z_1 dependence in z_{0b} and z_{0c} is relatively weak and that both give results very similar to z_{0a}, bearing in mind that it is $\ln z_0$ which is significant rather than z_0 itself. Both z_{0d} and z_{0e} values are substantially higher than z_{0a} for relatively low (10 m) values of z_1.

TABLE II

Further z_0^{eff} estimates for 'half-and-half' grid squares; $z_{0r}/z_{0s} = 10^2$, different z_1 levels

Ro	z_1 (m)	z_0^{eff} estimates (m)					
		z_{0m}	z_{0a}	z_{0b}	z_{0c}	z_{0d}	z_{0e}
10^6	10	0.100	0.159	0.170	0.136	0.455	0.316
	60	0.100	0.159	0.176	0.161	0.318	0.229
	300	0.100	0.159	0.182	0.176	0.258	0.194
10^7	10	0.010	0.0148	0.0163	0.0150	0.030	0.022
	60	0.010	0.0148	0.0168	0.0162	0.024	0.018
	300	0.010	0.0148	0.0172	0.0170	0.021	0.017

Ro values based on $V_g = 10\ \text{m s}^{-1}$, $f = 10^{-4}\ \text{s}^{-1}$ and z_{0m}.

7. The Effective Roughness Length for Flow Above a Surface with Sinusoidal Perturbations to $\ln z_0$

In addition to considering the 'patchwork quilt' problem, André and Blondin (1986) present results from a computation of the flow over a surface with sinusoidal perturbations to $\ln z_0$. Their model is two-dimensional and is essentially for the surface layer, in the sense that there are no Coriolis forces. Their formulation of the problem includes, however, two features to which we must draw attention:

(a) since there is no 'driving force', the flow decays with time and the computations of z_0^{eff} have to include corrections for non-steady-state effects;

(b) the flow situation considered is not truly periodic but consists of an area of uniform roughness followed by two wavelengths of sinusoidal $\ln z_0$ perturbation.

Walmsley *et al.* (1986) and Beljaars *et al.* (1987) have recently used flow over sinusoidally perturbed $\ln z_0$ as a test case for their linearized models of flow in complex terrain. They also compare their results with results from a third, nonlinear finite-difference model described by Taylor (1980). The flow situation considered in these papers is that of steady-state flow over an infinite plane with sinusoidal perturbations to $\ln z_0$. These models use a surface-layer formulation with the flow driven by an applied stress at the upper boundary. Ideally one would use a PBL formulation for the present application but we believe that the results of these models should still give some useful indication of the effect of sub-grid scale roughness modulation on the effective roughness for larger areas and avoid some of the potential problems inherent in André and Blondin's computations.

To determine the effective or apparent roughness length for this flow, we could set out to determine profiles at each point and then produce the average profile $\langle u(z) \rangle$. The models of Walmsley *et al.* and Beljaars *et al.* are, however, linearized in terms of the perturbations in $\ln z_0$ and the difference between $\ln z_{0a}$ and $\langle \ln z_0 \rangle$ will be a second-order quantity, which we cannot compute from the area-averaged profiles. We can, however, compute $\ln z_{0a}$ using Equation (3b), provided we assume that $\langle u(z) \rangle$ is

logarithmic in z, a reasonable hypothesis especially for large-wavelength roughness modulations.

In our notation the roughness variation can be written as

$$\ln z_0 = \langle \ln z_0 \rangle - q \cos(2\pi x/\lambda), \tag{16}$$

where λ is the wavelength of the modulation and the $\langle\ \rangle$ symbol now denotes an average over this wavelength. If we again set

$$\ln z_{0m} = \langle \ln z_0 \rangle, \tag{17}$$

then

$$z_0 = z_{0m} \exp(-q \cos 2\pi x/\lambda). \tag{18}$$

The roughness length minimum is located at $x = 0$ for $q > 0$.

This is essentially the same situation considered by André and Blondin but is truly periodic and uses a different notation for ease of comparison with Beljaars *et al.*'s work. With this distribution for $\ln z_0$, Equation (3b) gives

$$\begin{aligned} \ln z_{0a} &= \langle u_* \ln z_{0m} - q u_* \cos(2\pi x/\lambda) \rangle / \langle u_* \rangle \\ &= \ln z_{0m} - q \langle u_* \cos(2\pi x/\lambda) \rangle / \langle u_* \rangle . \end{aligned} \tag{19}$$

The linear models provide us with surface stress distribution of the form

$$\tau = \tau_0 + \tau_1,$$

where τ_0 is the applied stress at the top of the model and τ_1 is the $O(q)$ perturbation induced by the roughness variation. A simple balance of forces shows $\langle \tau_1 \rangle = 0$ for periodic flows. In Beljaars *et al.*'s linearized model, τ_1 is written in the form

$$\tau_1 = \tau_r \cos(2\pi x/\lambda) - \tau_i \sin(2\pi x/\lambda). \tag{20}$$

Also, on linearization, we can write

$$u_* = \tau_0^{1/2} \left(1 + \frac{1}{2} \frac{\tau_1}{\tau_o}\right). \tag{21}$$

Substitution of these expressions in (19) then gives, after some manipulation and averaging

$$\ln z_{0a} = \ln z_{0m} - \frac{q^2}{4} \left(\frac{\tau_r}{q \tau_0}\right) + \text{3rd order terms}. \tag{22}$$

The second-order correction term $(-\frac{1}{4}(q\tau_r/\tau_0)$, which is positive since $\tau_r < 0$ for $q > 0$, can be obtained from the linear theory in this case because of the form of Equation (3b) – in general second-order quantities cannot be obtained from the results of linear theories. In a somewhat similar way, we can also determine the ratio $\langle u_* \rangle / (\langle u_*^2 \rangle)^{1/2}$, another quantity which is second order in q, since the wavelength-averaged first- and

second-order perturbations to u_*^2 will be zero. The result is

$$\begin{aligned} \langle u_* \rangle &= \tau_0^{1/2}\left(1 - \frac{1}{8}\frac{\langle \tau_1^2 \rangle}{\tau_0^2}\right) + \text{3rd order terms} \\ &= \tau_0^{1/2}(1 - \tfrac{1}{16}(\tau_r^2 + \tau_i^2)). \end{aligned} \tag{23}$$

Inverting and squaring this gives a relation in the same form as Equation (10):

$$\langle u_*^2 \rangle = \langle u_* \rangle^2(1 + \tfrac{1}{8}(\tau_r^2 + \tau_i^2)). \tag{24}$$

TABLE III

Ratios of z_{0a}/z_{0m} and $\langle u_*^2 \rangle/\langle u_* \rangle^2$ for surface boundary-layer flow above sinusoidally modulated $\ln z_0$

λ/z_{0m}	$q = \ln 2$			$q = \ln 10$		
	ML	$E-\varepsilon$	FD	ML	$E-\varepsilon$	FD
(a) Ratio z_{0a}/z_{0m}						
10^3	1.083	1.042	1.071	2.405	1.580	2.145
10^4	1.053	1.034	1.050	1.764	1.442	1.723
10^5	1.038	1.028	1.037	1.510	1.349	1.506
10^6	1.029	1.023	1.030	1.375	1.283	n/a
10^7	1.024	1.019	1.025	1.293	1.235	n/a
(b) Ratio $\langle u_*^2 \rangle/\langle u_* \rangle^2$						
10^3	1.026	1.007	1.020	1.284	1.079	1.239
10^4	1.011	1.005	1.010	1.126	1.051	1.119
10^5	1.006	1.003	1.006	1.066	1.034	1.066
10^6	1.004	1.002	1.004	1.039	1.024	n/a
10^7	1.002	1.002	1.002	1.025	1.017	n/a

ML: Beljaars *et al.* (1987), mixing-length closure.
$E-\varepsilon$: Beljaars *et al.* (1987), $E-\varepsilon$ closure.
FD: Taylor (1980), turbulent kinetic energy equation, specified l.

Results based on Equations (22) and (24) are given in Table III for two values of q ($= \ln 2$ and $\ln 10$), five values of λ/z_{0m} and with two alternative closure schemes. Also given are results based on Taylor's (1980) nonlinear finite difference model. This has a closure intermediate between the mixing length (ML) and $E-\varepsilon$ forms in Beljaars *et al.*, but here gives results in good agreement with the Beljaars *et al.*'s ML model.

We note first of all that departures from unity of both ratios, z_{0a}/z_{0m} and $\langle u_*^2 \rangle/\langle u_* \rangle^2$ are always positive and decrease with increasing λ/z_0. The increases in z_0 are generally quite moderate and probably not significant for boundary-layer parameterization in large-scale models except for the lowest values of λ/z_{0m} considered.

The case considered by André and Blondin corresponds to $q = \ln 2$ and $\lambda/z_{0m} = 1.5 \times 10^6$. They calculate a ratio z_0^m/δ, equivalent to our z_{0b}/z_{0m}, as 1.067 for $z_1 = 5$ m. With $\lambda/z_{0m} = 10^6$, the present calculations give $z_{0a}/z_{0m} = 1.03$ and, from Equation (15) with $z_1 = 5$ m, $z_{0b}/z_{0m} = 1.04$. The discrepancy could be due to differences in the forms specified for mixing length or to the differences in flow configuration discussed earlier. It should, however, be stressed that both values are insignificant compared to the uncertainty usually present in our knowledge of the local z_0 field. It is interesting to note that André and Blondin's Figure 4 does show the effective roughness length perturbation, their A, increasing with height, z_1, near the surface and then decreasing above $z_1 \simeq 50$ m. In our view, the behaviour of their solution for $z_1 < 50$ m is qualitatively correct and in accord with our Equation (15). For $z_1 > 50$ m, we suspect that their result is influenced by the fact that the flow at this level is not in

a)

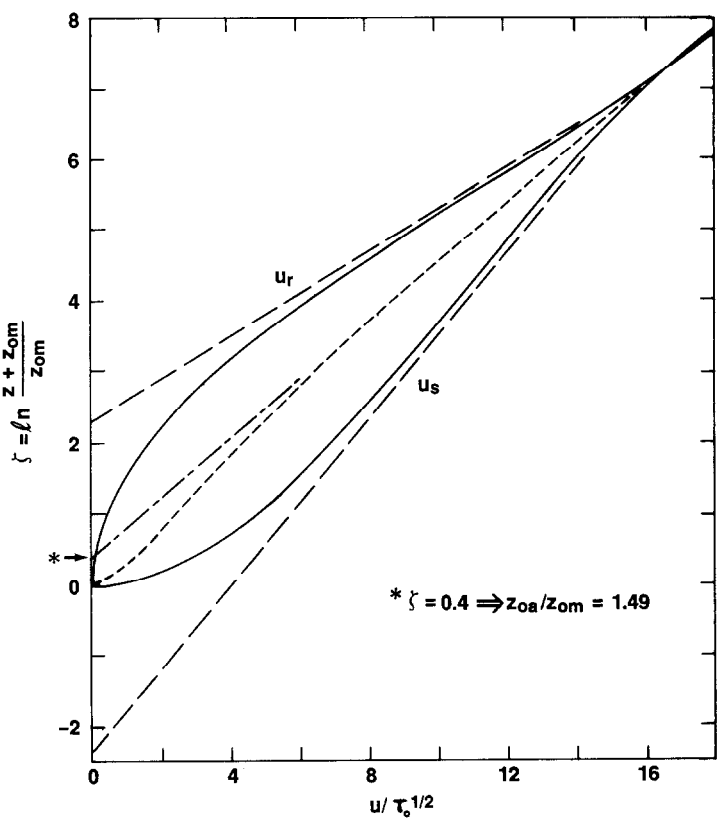

Fig. 3. Velocity profiles above a surface with sinusoidal perturbations in $\ln z_0$. Perturbation amplitude, $q = \ln 10$, (a) $\lambda/z_{0m} = 10^4$, (b) $\lambda/z_{0m} = 10^5$; ——— profiles over roughness extrema, u_r, u_s; – – – – average profile, $\langle u(z) \rangle$; — – — straight line extrapolation of $\langle u(z) \rangle$ for determination of z_{0a}; — — — schematic straight line profiles through $z_{0\,max}$, $z_{0\,min}$.

b)

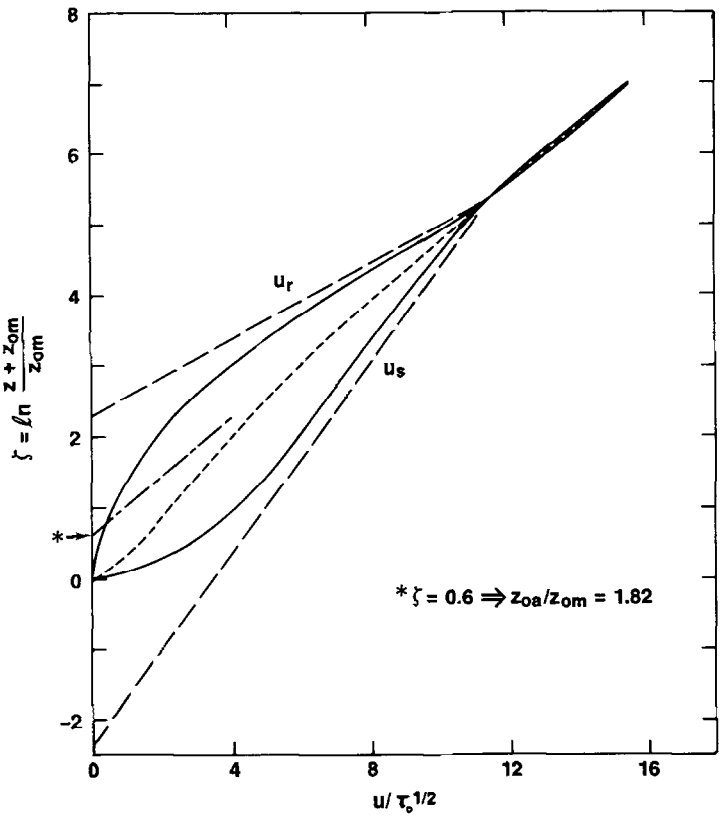

Fig. 3 (cont.).

a steady state. Simple order-of-magnitude estimates of the depth of flow affected after an elapsed time of 1500s support this suspicion.

To complete this discussion, we have used finite-difference model results to calculate sample average velocity profiles $\langle u \rangle$. These are plotted in Figure 3, together with profiles above the roughness maximum and minimum, for cases with $\lambda/z_0 = 10^4$ and 10^5 and with $q = \ln 10$. We can think of these as parameter values representing variations between short grass ($z_0 \sim 0.01$ m) and woodland or buildings ($z_0 \sim 1$ m) with a 1 km or 10 km wavelength – a sort of suburb with sports fields. The plots are of $u/\tau_0^{1/2}$ against $\ln((z + z_{0m})/z_{0m})$. This format forces the profiles to go through (0, 0) as the lower boundary condition but we can extrapolate from the profiles at upper levels where $z \gg z_0$ to calculate or graphically determine z_{0a}. These values are indicated on the figures and show $z_{0a}/z_{0m} = 1.82$ and 1.49, respectively, for the two cases with $\lambda/z_0 = 10^4$ and 10^5. These differ slightly from the values given in Table II based on the use of Equation (3b). The slight discrepancies could be due to the average profiles not being exactly of the form (3a) or to discretization error in the finite-difference model (which used a 20×25 mesh). The profiles confirm that, for $z \gg z_0$, the $\langle u(z) \rangle$ profile is approximately logarithmic, justifying, *a posteriori*, the use of Equation (3b).

The results of this section confirm André and Blondin's result that the effective roughness length for horizontally averaged flow over spatially varying z_0 is slightly greater than z_{0m}, and also provide estimates of the ratio z_{0a}/z_{0m} for two values of q and a range of values of λ/z_{0m}. Our interpertation of them, in contrast to that made by André and Blondin, is that the z_{0a} values computed are not significantly different from z_{0m} and, furthermore, that the stress correction factor, $\langle u_*^2 \rangle / \langle u_* \rangle^2$ is not significantly different from 1.0 in most cases, relative to other errors and uncertainties in the treatment of the boundary layer in large-scale models. Doubling the largest value of q used in Table III would give more significant differences but clearly strains the validity of the linear model results. However, let us consider what happens with $q = \ln 100$ and $\lambda/z_{0m} = 10^6$ (roughness varying from $z_0 = 0.0001$ m to 1 m with a wavelength of 10 km). This is quite an extreme case but somewhat representative of the lakes and forests of parts of Canada. Beljaars *et al.*'s (1987) ML model predicts $z_{0a}/z_{0m} = 3.57$ and $\langle u_*^2 \rangle / \langle u_* \rangle^2 = 1.16$. This suggests that, for these extreme cases, the assumptions made in earlier sections of the paper concerning the neglect of transition zone effects could warrant closer inspection.

8. Discussion

The primary intent of this research note is to provide an alternative view of André and Blondin's assertions that (i) 'the ERL (effective roughness length) is mostly determined by the roughest elements in the averaging domain', (ii) 'the ERL increases as the first level of the numerical model (z_1) gets close to the surface', and (iii) 'it (z_0^{eff}) is not a quantity with unambiguous physical significance'. We have aimed to show that assumptions made in parts of André and Blondin's analysis lead to an overestimation of (i) and that in most cases a simple average of the logarithm of the local surface roughness over a grid square will yield an adequate estimate for $\ln z_0^{\text{eff}}$. We also suggest a 'correction' term based on the variance of $\ln z_0$ within the grid square (Equation (6b)) and using relationships based on PBL similarity theory. This correction does bias the average towards the larger $\ln z_0$ values in qualitative accord with André and Blondin's result but to a rather lesser extent. For our preferred definition of an effective roughness length, z_{0a}, there is no dependence on the grid level, z_1, and with our second choice, z_{0b}, there is a weak *decrease* with decreasing z_1. This contrasts with the behaviour given by (ii) above and also with values, z_{0d}, based on grid-square averages of the drag coefficient $C_D(z_1)$. Results based on numerical models of flow above a surface with sinusoidal perturbations to $\ln z_0$ are discussed. These confirm André and Blondin's result that $z_0^{\text{eff}} > z_{0m}$ for such flows but our interpretation is that these differences are small except in extreme cases. The analyses given here are not the final word on z_0^{eff} but do, we believe, provide some useful guidance in relating effective roughness lengths for large-scale models to the sub-grid-scale micrometeorological roughnesses. There is still some ambiguity in the specification of z_0^{eff} but it is less than André and Blondin imply.

We have not addressed the problems associated with abrupt transition zones, the

representation of the drag due to flow over sub-grid scale topographic features or the potentially very difficult problems of boundary-layer parameterization in areas with spatial inhomogeneities in thermal stratification (see, for example, Smith and Carson, 1977). Some progress may be possible by using detailed boundary-layer models to study the flow in either generic or specific areas of complex terrain corresponding to single grid squares of larger-scale models. In particular, we believe that Beljaars *et al.*'s (1987) MSFD model, or an extension theorof, has the potential for this type of application and we hope to pursue this area of research in the future.

Acknowledgements

Norman McFarlane and Yves Delage of AES made helpful comments on the manuscript while correspondence and discussions with Dave Carson, Paul Mason, and Jon Wieringa have helped in the formulation of some of the ideas.

Appendix 1. Similarity Theory Forms for the $u_*(\ln z_0)$ Relationship

PBL similarity theory predicts the relationship between surface friction velocity and roughness Rossby number to be

$$\ln\left(\frac{u_*}{V_g}\,\mathrm{Ro}\right) = B + \left[\frac{k^2}{(u_*/V_g)^2} - A^2\right]^{1/2}. \tag{A1}$$

(See, for example, McBean, 1979, p. 45, but beware the missing + sign!) Here k is the von Karmán constant which we shall take as 0.4. A and B are constants for neutral stratification but can also be considered as functions of the stability parameter $\mu = ku_*/fL$ where L is the Monin–Obukhov length, for non-neutral cases. Even for neutral conditions they are not very well determined. We shall use $A = 4$, $B = 2$ as 'typical' values for calculations of the curves shown in Figure 2. Differentiating (A1) with respect to $\ln z_0$ and rearranging terms leads to the relationship

$$a_1 = \frac{1}{u_*}\frac{\mathrm{d}u_*}{\mathrm{d}(\ln z_0)} = \frac{F}{A^2 + F^2 + F} = \frac{F}{F + k^2 V_g^2/u_*^2} \tag{A2}$$

where

$$F = \left(\ln\frac{u_*}{V_g} - B + \ln\frac{V_g}{fz_0}\right).$$

Note that this is only valid if μ is regarded as fixed, as it would be for neutral conditions. There will be additional terms involving $\mathrm{d}A/\mathrm{d}\ln z_0$ and $\mathrm{d}B/\mathrm{d}\ln z_0$ if the stability parameter is an implicit function of $\ln z_0$.

Further differentiation and manipulation under the same assumptions leads to

$$a_2 = \frac{1}{2u_*}\frac{\mathrm{d}^2u_*}{\mathrm{d}(\ln z_0)^2} = \frac{(2F+1)(A^2+F^2)a_1 - A^2}{2(A^2+F^2+F)^2}. \tag{A3}$$

References

André, J.-C. and Blondin, C.: 1986, 'On the Effective Roughness Length for Use in Numerical Three-Dimensional Models', *Boundary-Layer Meteorol.* **35**, 231–245.

Beljaars, A. C. M., Walmsley, J. L., and Taylor, P. A.: 1987, 'A Mixed Spectral, Finite Difference Model for Neutrally Stratified Boundary-Layer Flow over Roughness Changes and Topography', *Boundary-Layer Meteorol.* **38**, 273–303.

Fiedler, F. and Panofsky, H. A.: 1972, 'The Geostrophic Drag Coefficient and the Effective Roughness Length', *Quart. J.R. Meteorol. Soc.* **98**, 213–220.

Jensen, N.-O.: 1978, 'Change of Surface Roughness and the Planetary Boundary-Layer', *Quart. J. R. Meteorol. Soc.* **104**, 351–356.

McBean, G. A. (ed.): 1979, *The Planetary Boundary-Layer*, WMO – No. 530, World Meteorological Organization, Geneva, 201 pp.

Smith, F. B. and Carson, D. J.: 1977, 'Some Thoughts on the Specification of the Boundary-Layer Relevant to Numerical Modelling', *Boundary-Layer Meteorol.* **12**, 307–330.

Taylor, P. A.: 1969a, 'On Wind and Shear Stress Profiles above a Change in Surface Roughness', *Quart. J.R. Meteorol. Soc.* **95**, 77–91.

Taylor, P. A.: 1969b, 'The Planetary Boundary-Layer above a Change in Surface Roughness', *J. Atmos. Sci.* **26**, 432–440.

Taylor, P. A.: 1980, 'Some Recent Results from a Numerical Model of Surface Boundary-Layer Flow over Hills', in J. C. Wyngaard (ed.), *Workshop on the Planetary Boundary-Layer*, Amer. Meteorol. Soc., Boston, pp. 150–157.

Walmsley, J. L., Taylor, P. A., and Keith, T.: 1986, 'A Simple Model of Neutrally Stratified Boundary-Layer Flow over Complex Terrain with Surface Roughness Modulations (MS3DJH/3R)', *Boundary-Layer Meteorol.* **36**, 157–186.

Wieringa, J.: 1986, 'Roughness Dependent Geographical Interpolation of Surface Wind Speed Averages', *Quart. J. R. Meteorol. Soc.* **112**, 867–889.